

Home Search Collections Journals About Contact us My IOPscience

Improving Mechanical Properties of Carbon Nanotube Fibers through Simultaneous Solid-State Cycloaddition and Crosslinking

This content has been downloaded from IOPscience. Please scroll down to see the full text.

Download details:

IP Address: 128.219.49.14

This content was downloaded on 27/02/2017 at 11:30

Manuscript version: Accepted Manuscript

Kang et al

To cite this article before publication: Kang et al, 2017, Nanotechnology, at press: https://doi.org/10.1088/1361-6528/aa6223

This Accepted Manuscript is: © 2017 IOP Publishing Ltd

During the embargo period (the 12 month period from the publication of the Version of Record of this article), the Accepted Manuscript is fully protected by copyright and cannot be reused or reposted elsewhere.

As the Version of Record of this article is going to be / has been published on a subscription basis, this Accepted Manuscript is available for reuse under a CC BY-NC-ND 3.0 licence after a 12 month embargo period.

After the embargo period, everyone is permitted to use all or part of the original content in this article for non-commercial purposes, provided that they adhere to all the terms of the licence https://creativecommons.org/licences/by-nc-nd/3.0

Although reasonable endeavours have been taken to obtain all necessary permissions from third parties to include their copyrighted content within this article, their full citation and copyright line may not be present in this Accepted Manuscript version. Before using any content from this article, please refer to the Version of Record on IOPscience once published for full citation and copyright details, as permissions will likely be required. All third party content is fully copyright protected, unless specifically stated otherwise in the figure caption in the Version of Record.

When available, you can view the Version of Record for this article at: http://iopscience.iop.org/article/10.1088/1361-6528/aa6223

Improving Mechanical Properties of Carbon Nanotube Fibers through Simultaneous Solid-State Cycloaddition and Crosslinking

Xinyi Lu¹, Nitilaksha Hiremath², Kunlun Hong³, Maria C. Evora^{1,4}, Victoria H. Ranson⁵, Amit K. Naskar⁶, Gajanan S. Bhat², Nam-Goo Kang^{1,*} and Jimmy W. Mays^{1,*}

Abstract

Individual carbon nanotubes (CNTs) exhibit exceptional mechanical properties. However, difficulties remain to fully realize these properties in CNT macro-assemblies, because of the sliding past one another resulting from the weak inter-tube forces. Herein, a simple solid-state reaction is presented that enhances the mechanical properties of carbon nanotube fibers (CNTFs) through simultaneous covalent functionalization and crosslinking. This is the first chemical crosslinking proposed without involvement of catalyst or byproducts. The specific tensile strength of CNTF obtained from the treatment employing a benzocyclobutene-based polymer is improved by 40%. Such improvement can be attributed to reduced voids, impregnation of polymer, and the formation of covalent crosslinks. This methodology is confirmed using both multiwalled nanotube (MWNT) powders and CNTF. Thermogravimetric analysis, differential scanning calorimetry, X-ray photoelectron spectroscopy, and transmission electron microscopy of the treated MWNT powders confirm the covalent functionalization and formation of intertube crosslinks. This simple one-step reaction can be applied to industrial-scale production of high-strength CNTFs.

Keywords: Carbon Nanotube Fiber, One-step Crosslinking, Chemical Post-treatment

¹Department of Chemistry, University of Tennessee, 1420 Circle Dr., Knoxville, TN 37996, USA

²Department of Materials Science and Engineering, University of Tennessee, 1508 Middle Dr., Knoxville, TN 37996, USA

³Center for Nanophase Materials Sciences Division, Oak Ridge National Laboratory, P.O. Box 2008, Oak Ridge, TN 37831, USA

⁴Institute for Advanced Studies- IEAV/DCTA, São Jose dos Campos, SP 12228, Brazil

⁵Department of Chemistry and Biochemistry, The University of Texas at Dallas, 800 W Campbell, BE26, Richardson, TX 75080, USA

⁶Materials Science and Technology Division, P.O. Box 2008, Oak Ridge, TN 37831, USA

^{*} Corresponding authors. Phone: +1 865 974 0747 Fax: +1 865 974 9332 E-mail address: nkang1@utk.edu (N.-G. Kang) and jimmymays@utk.edu (J. W. Mays)

1. Introduction

Carbon nanotube fibers (CNTFs) have received much attention for their promising applications in actuators[1], supercapacitors [2], and light-weight magnetic shields [3], but key challenges remain to realize their full potential in terms of mechanical properties [4-6]. The tensile strength of pristine CNTF reported thus far vary from 0.15-8.8 GPa, depending on the type of CNTs used, their packing, and associated processing [7-9]. Even the highest reported strength (8.8GPa) [10] is only a fraction of that of the individual carbon nanotube (CNT) building blocks, which is on the order of 100 GPa [11].

CNTFs are fabricated through various means resembling the traditional fiber spinning techniques, such as wet spinning from CNT solutions [12, 13], dry spinning from vertically aligned CNT arrays [7, 14], and direct spinning of aerogels from chemical vapor deposition(CVD) reactors [15]. The integrity and properties of as-spun CNTF rely on weak Van der Waal's interactions and low friction forces present between components [16-18]. As a result, upon tensile loading of the fiber, the CNT building blocks and their bundles slide past one another causing inefficient load transfer from macroscopic CNTFs down to the individual tubes [18, 19]. Numerous post treatment methods have been developed to enhance the load transfer and improve the mechanical properties of CNTFs, such as solvent densification [8, 20], polymer infiltration [21, 22], and crosslinking [23-30], but each with its limitations.

There are two approaches reported in the literature which claimed to achieve "crosslinking" or CNTFs: (i) infiltration of functional monomer/polymer in CNTF followed by curing without involving reaction with CNTs (should be regarded as "consolidated") [24-27], and (ii) covalent crosslinking between CNTs with or without chemical functionalization [23, 28-32]. In the first approach, curing of the infiltrated material such as catecholamine polymer [24], photoreactive diene [25], epoxy [27], and polyacrylonitrile [26], successfully trapped the CNTs in a rigid network and yielded mechanical interlocking. In the second approach, crosslinking shall be achieved by introducing covalent bonds within the CNTF. Simulations suggest that introducing

covalent crosslinks to CNTF should improve their mechanical strength by 1-2 orders of magnitude [33], However, only very few reports demonstrated the covalent crosslinking of CNTFs on the macroscopic scale, either through chemical functionalization [29-31], or irradiation [23, 28, 32]. None of the reports have reached the predicted improvement, and most of them employed tedious process.

Covalent crosslinking of CNTFs using chemical functionalization is typically achieved through multiple steps in solution: a surface functionalization on CNT to introduce an active moiety followed by reaction with a multi-functional crosslinker or coupling of the functional groups [29, 30]. Despite the increase in mechanical strength observed in CNTFs treated by these chemically crosslinking methods, multiple steps of functionalization were required, which potentially means repetitive reactions, rinsing and drying. Intramolecular cross-dehydrogenative coupling has been used as a single-step treatment for CNTFs [31], but the reaction occurred in solution requiring catalysts, which may create obstacles to potential scale-up. Moreover, many of the results of these treatments were reported only in terms of traditional tensile strength, which is less comparable to other fibers than density normalized specific strength considering irregularity of the cross-sections.

Herein, we report a novel one-step solid-state chemical treatment using a benzocyclobutene (BCB) based polymer. This is a facile approach with BCB functional groups covalently attached onto CNT walls while these groups react with each other simultaneously to form stable covalent bonds. These chemical crosslinks between CNTs are visualized by transmission electron microscopy (TEM). Effect of the designed chemical crosslinking process on the tensile properties of CNTF is discussed both in terms of the traditional method and the density normalized method.

- 2. Experimental
- 2.1 Synthesis of Polymer Linker Poly(styrene-r-4-vinylbenzylcyclobutene) (PS-VBCB)

A series of the PS-VBCB polymer linkers with varying monomer ratio was synthesized by anionic polymerization [34]. In the preparation of a typical PS-VBCB, the monomers, 4-vinyl benzocyclobutene (4-VBCB, synthesized as previously reported [35]), and styrene (Fisher Scientific,>99%) were purified by exposure to and distillation from calcium hydride (Acros Organics, 93%) and dibutylmagnesium (Sigma Aldrich, 1.0M in heptane), successively, then diluted in anhydrous THF (Fisher Scientific, ACS grade) to ~0.8M and sealed in glass ampules. A hand-crafted all-glass reactor was equipped with an ampule containing sec-butyl lithium (Acros Organics, 0.218 mmol, 1.3M in hexanes) as the initiator, an ampule containing a mixture of diluted monomers (26.9 mmol styrene and 6.9 mmol 4-VBCB) and an ampule of purified methanol (Fisher Scientific, 1mL, >99.5%). After the reactor was flame-sealed from the vacuum line, the initiator and the monomer ampules were cut open and allowed to polymerize for 30 minutes at -78°C before quenching with methanol. The mixture was released from the reactor and precipitated in methanol (500 mL) with vigorous stirring (3 times). Finally, the polymer was dried in a vacuum oven overnight at room temperature to afford a white powder.

2.2 Crosslinking MWNT powder

MWNT powder (>99%) was purchased from Cheap Tubes Inc., and used as received. In a small beaker, MWNT powder was immersed in PS-VBCB solution (5 mL, 90 wt.% in toluene) and the solvent was allowed to evaporate. The mixture was dried in vacuum for 2 hours to remove any residual solvent, which reduced the distance between the CNT bundles by the capillary effect. A sample at this point, denoted as PS-VBCB infiltrated MWNT, was then heated in N₂ for 24 hours to ensure the crosslinking reaction is complete. The crosslinked MWNT appeared as sheering flakes due to rigid crosslinking between adjacent CNT bundles. Finally, the sample was rinsed with copious THF and toluene to remove unreacted PS-VBCB. In order to prove that rinsing effectively removed most of the residual linker, a control sample was prepared by immersing MWNT powder into 90 wt.% PS-VBCB solution in toluene and washed by the same process without heat-induced crosslinking.

2.3 Crosslinking CNTF

CNTF was produced by University of Cincinnati through a proprietary process and were used as received. CNTF were treated with the solution of PS-VBCB in toluene at lower concentration (0.1 wt.%), because low linker content is desired to retain high purity in the resultant CNTF. The as-spun CNTFs, noted as pristine, was immersed in PS-VBCB solution (0.1 wt.% in toluene) for 1 hour to enable effective infiltration of the linker into the CNTF. This step is readily applicable in industry by simply adding a bath in the CNTF spinning process. The fiber was then removed from the solution and dried under vacuum at 60 °C for 12 hours. A sample at this stage was denoted as PS-VBCB infiltrated CNTF. A sample that was further heated at 250 °C in N₂ for 4 hours while being stretched to straight is named as PS-VBCB crosslinked CNTF. Both PS-VBCB infiltrated and crosslinked CNTF contained up to 7 wt.% of linker determined by gravimetric analysis.

2.4 Characterizations

Thermogravimetric analysis (TGA) (Q50, TA Instrument) was used to analyze the content of linker on treated CNT, at a ramp rate of 10 °C/min to 1000 °C in nitrogen. The thermal behavior of the crosslinking reaction was monitored by differential scanning calorimeter (DSC) (Q2000, TA Instrument) at 5 °C/min from 80 °C to 280 °C. The chemical characteristic of CNTs was evaluated using X-ray photoelectron spectroscopy (XPS) (K-Alpha, Thermo Scientific). Data were collected and analyzed using the Advantage data system (v.4.61). C 1s high resolution core level spectra were recorded at 50 eV pass energy. The atomic concentrations of the detected elements were calculated using integral peak intensities. Inter-tube crosslinking was visualized by transmission electron microscopy (TEM) (Libra 200 MC, Zeiss). The surface morphology and internal structure of CNTF were investigated by focused ion beam scanning electron microscope (FIB-SEM) (Auriga, Zeiss). Gallium ion was used as FIB source to mill the cross sections of the CNTFs inside the SEM chamber. The tensile properties of CNTFs were assessed on a MTS single filament tensile tester, with gauge length of 25mm and extension rate

of 0.2mm/min. The diameters of the fibers were measured with $500\times$ optical microscope and used to calculate the ultimate strength (breaking force/ $(0.25\pi d^2)$), since the shape of CNTF is almost perfectly cylintrical (see **Fig.4** (a-c)). Eight specimens from each yarn sample were tested and the average of the results was reported. In addition, density-normalized tensile properties were derived from breaking force (N) and linear density (tex). The densities of the pristine, toluene densified, PS-VBCB infiltrated, and PS-VBCB crosslinked CNTF are 0.2, 0.4, 0.4, and 0.5 g/cc, respectively, calculated from dividing tensile strength by specific strength.

- 3. Results and discussion
- 3.1 Establishment of covalent functionalization and crosslinking

In this work, benzocyclobutene (BCB) chemistry was applied. Upon heating, the 4-membered ring of BCB transforms into reactive o-quinodimethane intermediate that can couple with sp² carbons of aromatic systems through [4+2] Diels-Alder (D-A) cycloaddition,[36, 37] as illustrated in Fig. 1(a). BCB-containing materials can be widely used to covalently functionalize carbon nanomaterials for several advantages, such as 1) statistical distribution of functional groups on the CNT wall instead of favoring tube ends and defect sites, 2) no catalyst required, and 3) no release of any small molecules during the reaction. For our purpose, PS-VBCB random copolymer was prepared via anionic polymerization and characterized by size exclusion chromatography (SEC) and nuclear magnetic resonance (NMR) (see Figure S1 and S2 in the supporting information). The non-reactive styrene units were added to the copolymer to suppress the inevitable intramolecular reaction between BCB units, which leads to formation of collapsed polymer nano particles[35] that negatively affects mechanical properties of the fiber. However, polystyrene itself is a relatively rigid polymer, and the mechanical properties of CNTF can hardly reach the optimum if too much styrene is present. Therefore, a series of PS-VBCB with varying monomer ratio were synthesized and applied to CNTF to study the effect of monomer ratio on the mechanical properties of crosslinked CNTF, as in Fig. S3. The ratio of styrene to BCB leading to the best result is approximately 4:1 and an illustration of the

chemical structure is shown in **Fig. 1**(b). As schematically shown in **Fig. 1**(c-e), our approach involves infiltration of the polymer linker, PS-VBCB, into CNT materials followed by thermally induced reaction of BCB units with the sp² carbons on CNT walls. The polymer backbone acts as inter-tube crosslinks when BCB moieties on the same polymer chain grafts onto adjacent CNTs. In addition, the coupling of BCB with BCB generates a reticulate network that might also contribute to inter-tube crosslinks (**Fig. 2**).

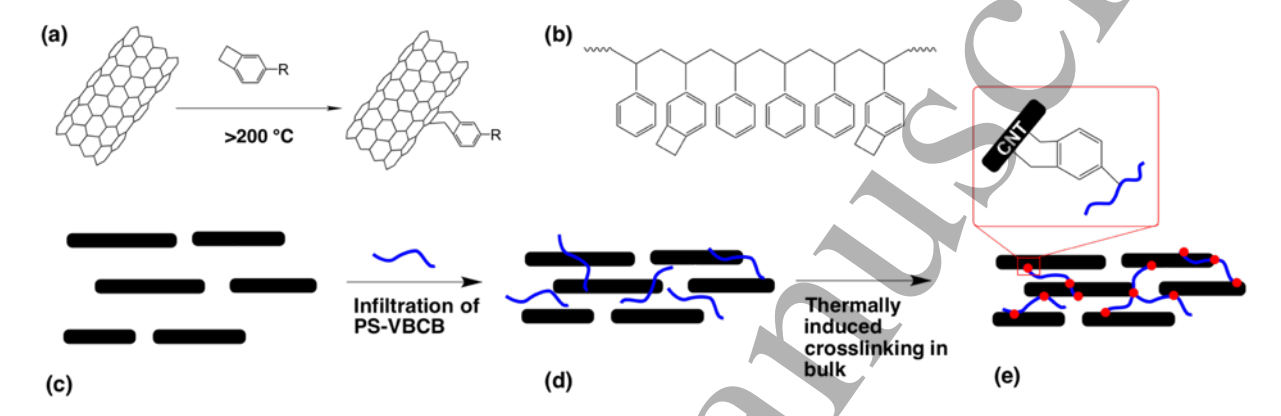


Fig. 1 (a) D-A cycloaddition of BCB derivatives with CNT; (b) Chemical structure of PS-VBCB; (c-e) Preparation of PS-VBCB crosslinked CNTF by infiltration and thermally induced reaction, and the CNTFs at each stage during the crosslinking process denoted as (c) Pristine CNTF; (d) PS-VBCB infiltrated CNTF; (e) PS-VBCB crosslinked CNTF

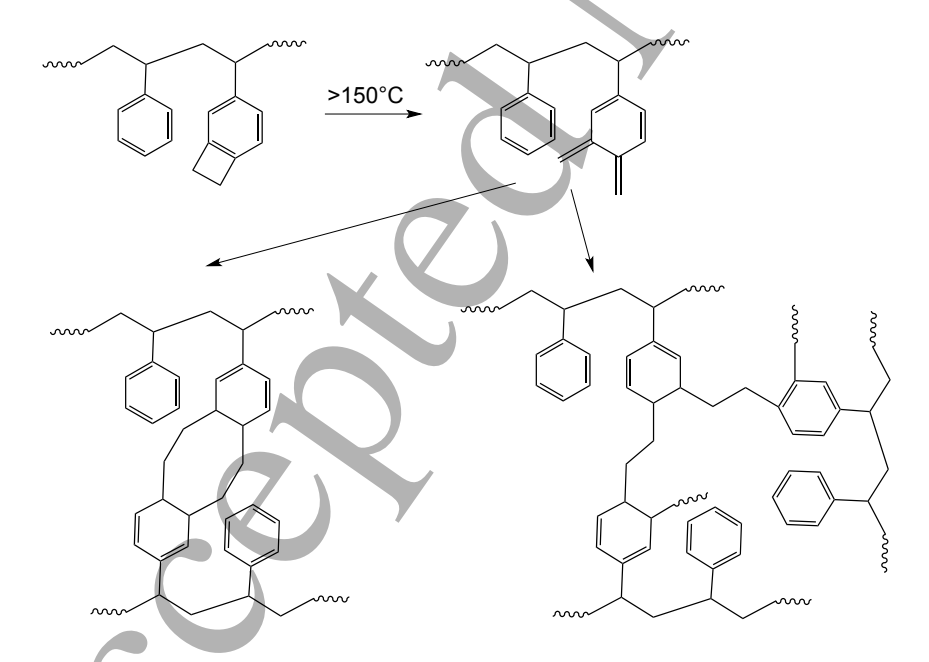


Fig. 2 Reaction between BCB moieties to form cyclooctadiene (left) and crosslinked polymer (right)

Given that a meter of the CNTF used in the study weighs only 0.7 mg, it is a big challenge to apply characterization methods that require milligrams of sample. In order to fully demonstrate the chemistry and support the proposed mechanism, bulk multi-walled nanotube (MWNT) powder samples were crosslinked and investigated for such characterizations, since CNT powder is very close to CNTFs in terms of chemical reactivity since they are both composed of MWNT bundles.

The thermogravimetric analysis (TGA) [Fig. 3(a)] reveals a single-step 63% weight loss at around 400 °C for the crosslinked MWNT. This is attributed to the thermal decomposition of reticulate crosslinked PS-VBCB network. Uncured PS-VBCB infiltrated MWNT was rinsed with solvent to obtain physically adsorbed PS-VBCB on the MWNT (control MWNT). Such sample shows 3 wt.% PS-VBCB sorption on MWNT surface by TGA. The reacted portion of BCB linkers went through either cycloaddition with MWNT or with other BCB moieties to form crosslinks. In addition, the cycloaddition and crosslinking reaction of MWNT and PS-VBCB was verified through differential scanning calorimetry (DSC) by heating the PS-VBCB infiltrated MWNT in-situ, as shown in Fig. 3(b). During the heating ramp in the first cycle, two signals were clearly observed at 100 °C and 200 °C. The endothermic step transition occurred near 100 °C is attributed to the glass transition of PS-VBCB where segmental movement of polymer chains is unlocked. The wide exothermic peak initiated at around 200 °C is associated with activation of BCB units for further cycloaddition and crosslinking with MWNT. As the sample was heated again, both of the signals disappeared. Absence of the glass transition confirms transformation of PS-VBCB to a crosslinked reticulate structure and loss of polymer segmental movement. Also, BCB has fully reacted prior to the second heat ramp due to the absence of an exothermic peak at 200 °C in the second cycle. These thermal characterizations by TGA and DSC provide solid evidence of BCB-induced crosslinking.

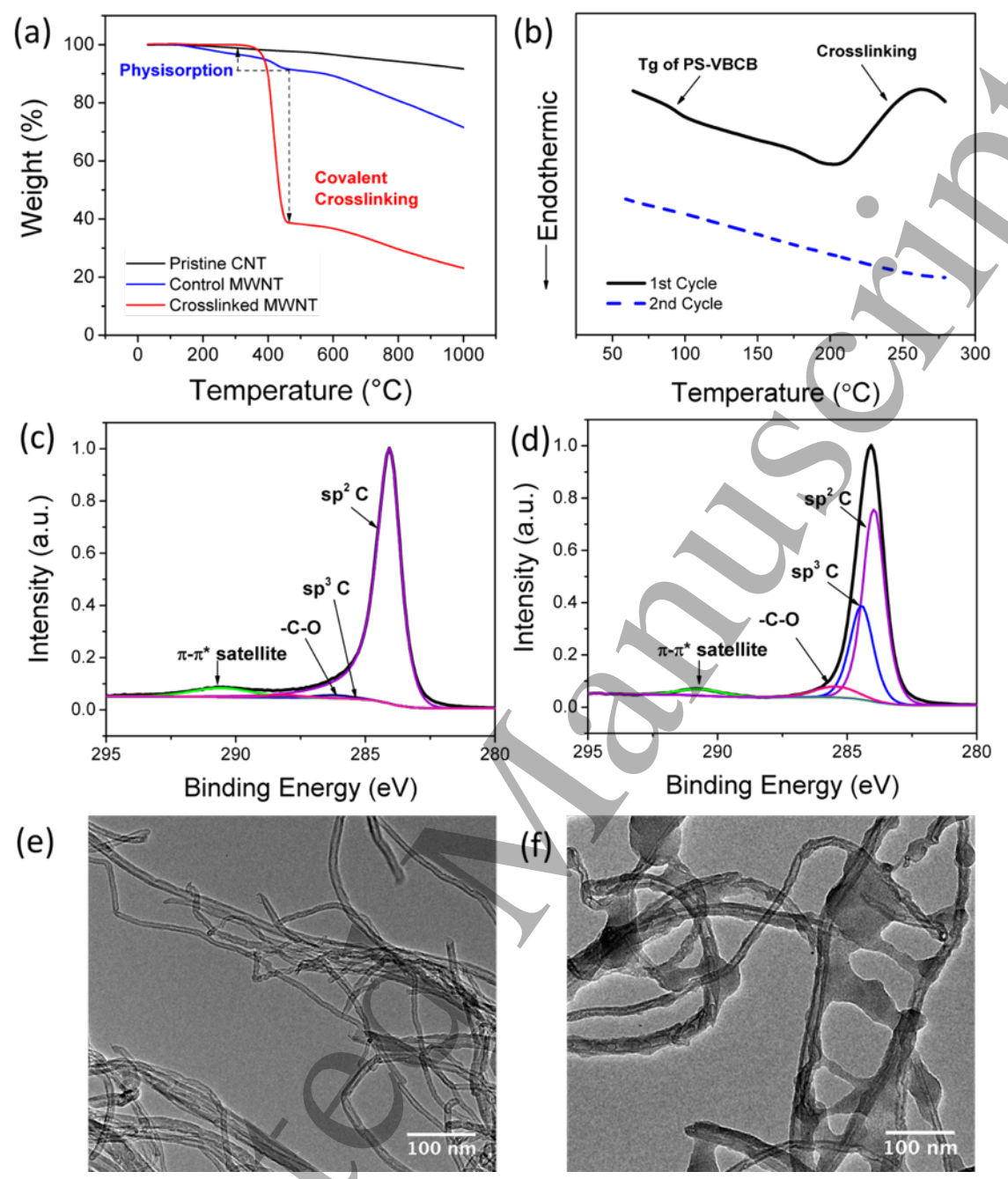


Fig. 3 Thermal analyses of treated MWNT powder: (a) TGA overlay of PS-VBCB crosslinked MWNT with pristine and control MWNT; (b) DSC curve of PS-VBCB infiltrated MWNT. XPS of (c) control MWNT and (d) crosslinked MWNT. TEM image of (e) Pristine MWNT and (f) PS-VBCB crosslinked MWNT

Covalent functionalization of BCB onto MWNTs through D-A cycloaddition is supported by X-ray photoelectric spectroscopy (XPS) results. Again, MWNT powder was used to demonstrate the reactivity of C=C on CNTs with PS-VBCB, and the result can be projected to the reaction with CNTs on CNTF. XPS results presented in **Fig. 3 (c-d)** show the high-resolution C 1s spectra of PS-VBCB infiltrated MWNTs and crosslinked MWNTs, respectively.

In order to identify differences in the chemical states of carbon in these samples, deconvolution of the C 1s curve was performed and five characteristic peaks were revealed. Binding energy of 284.3, 284.8, 286.5 288.5, and 291.3 eV correspond to sp^2 -hybridized carbon, sp^3 -hybridized carbon, C-O, C=O, and π - π * satellite signals. These peaks were fitted with a combination of Gaussian-Lorentzian functions and integrated to quantify the contribution of each component. The relative intensity of sp^2 and sp^3 carbons is a good indication of covalent functionalization on MWNT. Since the reaction between BCB groups themselves (**Fig. 2**) does not induce any changes in the chemical status of carbon on MWNT, lower sp^2 and higher sp^3 in the crosslinked MWNT suggests conversion of C=C unites on the CNT wall to C-C due to cycloaddition reaction with BCB. Negligible signals of C-O and C=O are attributed to defects on MWNT and adventitious carbon. The π - π * satellite signal is characteristic of aromatic structures which can be correlated to graphitic structure on MWNT.

The pristine MWNT and inter-tube crosslinking in the crosslinked samples were visualized via transmission electron microscopy (TEM), as shown in **Fig. 3**(f). In contrast to the morphology of pristine MWNT in **Fig. 3**(e), a near-homogeneous polymer layer was observed covering the MWNTs crosslinked with PS-VBCB [**Fig. 3**(f)]. This suggests that the BCB functional groups were statistically distributed on the MWNTs, instead of being isolated at tube ends or defect sites. In addition to the layer covering the wall, polymeric material also formed inter-tube linkages, resembling the horizontal bars on a ladder.

3.2 Effect of the process on the morphology of CNTF

After validating our novel strategy using MWNT powder, we then studied the effect of the crosslinking process on the morphology and mechanical properties of CNTFs. The surface structures of pristine CNTF with a diameter of $67.3\pm0.9~\mu m$, PS-VBCB infiltrated CNTF with $37.1\pm1.1~\mu m$, and PS-VBCB crosslinked CNTFs with $36.4\pm3.5~\mu m$ were observed under SEM at low magnification, as shown in **Fig. 4**(a-c). The CNTs were mostly aligned to the axis of the fiber at a twist angle. While the pristine CNTF exhibits loosely packed structure, PS-VBCB

infiltrated and PS-VBCB crosslinked CNTF were condensed to smaller dimensions, primarily due to solvent evaporation after infiltration of linker. Intuitively, introducing crosslinks within the fibers can cause slight shrinkage in diameter, such as direct inter-tube linkages caused by irradiation[23, 32]. However, in many treatments crosslinking CNTF, especially chemical crosslinking methods that introduce functional groups as linkages, no obvious decrease in diameters have been reported due to crosslinking or curing [23, 24, 29, 31]. In this study, the average diameters of PS-VBCB infiltrated fiber before and after heating [Fig. 4(b) and Fig. 4(c), respectively] are very similar, but the error range of the diameters increased. This is due to low percentage of PS-VBCB infiltrated into the fiber (<7%), and the crosslinking reactions occur locally and irregularly, causing some area to shrink and others to swell. Furthermore, due to low void content in infiltrated CNTF, little space is left for crosslinking to further reduce the varn diameter. In addition, the impregnated polymer in [Fig. 4(b)] created a smooth layer on the surface of the fiber as compared with the less compact structure observed in the pristine sample [Fig. 4(a)]. After thermally induced crosslinking, PS-VBCB collapsed into a reticulate structure, leading to an increase in surface waviness of the fibers [Fig. 4(c)]. Higher magnification images Fig. 4(d-f) provided further details on the surface morphology. In contrast to pristine CNTF in Fig. 4(d), lower void content was found in Fig. 4(e-f), which is responsible for the difference in the diameters of these samples. Given their close proximity to each other, CNTs and CNT bundles in the densified fiber can easily get in contact with PS-VBCB to enable inter-tube/inter-bundle crosslinking. Consistent with observations from Fig. 4(a-c), a continuous layer of polymer is shown on the CNTF in Fig. 4(e) due to infiltration of PS-VBCB; subsequent heating has introduced irregularities to the surface by turning the continuous polymer cover on CNTs into rigid network that joins the CNTs into large bundles [Fig. 4(f)].

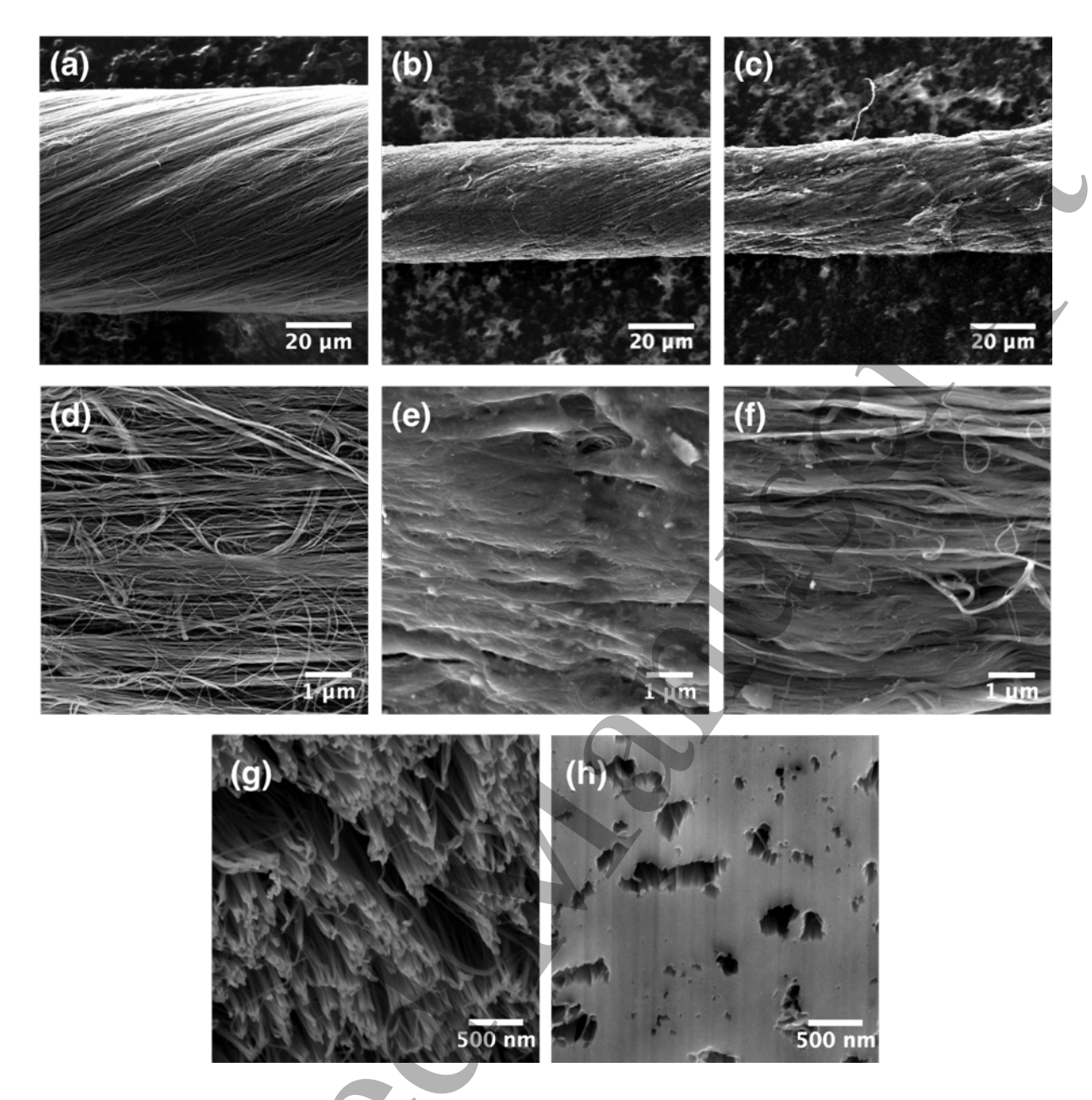


Fig. 4 Low magnification SEM images of (a) Pristine, (b) PS-VBCB infiltrated, and (c) PS-VBCB crosslinked CNTF; high magnification SEM images of (d) Pristine, (e) PS-VBCB infiltrated, and (f) PS-VBCB crosslinked CNTF; FIB-milled cross-section of (g) Pristine, and (h) PS-VBCB infiltrated CNTF

The internal structure of the CNTFs was investigated by imaging at the focused ion beam (FIB)-milled cross-sections that are 10 μ m deep [Fig. 4(g-h)]. Again, the pristine fiber was composed of mostly empty spaces, as in Fig. 4(g). After infiltration of the linker and evaporation of solvent, the CNTs were almost "welded" together, only exhibiting occasional vacancies [Fig. 4(h)].

Note that the diameter of the PS-VBCB infiltrated CNTF was around 37 μ m, thus the 10 μ m-deep cut should fairly represent most of the cross-sectional area. This showed that our polymer was infused effectively towards the center of the fiber during infiltration for 1 hour.

3.3 Effect of the process on mechanical properties of CNTF

There are several methods to report the mechanical properties of CNTF[38], and the two most commonly used ones were discussed below. The traditional tensile strength can be obtained from assuming cylindrical shape of the fiber, where the cross-sectional area $A = 0.25\pi d^2$ [24, 26, 27, 29, 31].

$$\sigma = \frac{F}{A}$$

Another approach reports the specific strength in GPa·SG⁻¹ (equivalent to N/tex) in terms of force (N) per the linear density of the fiber (g/km). The specific strength makes it easier to compare between different types of fibers.

$$\sigma^* = \frac{N}{tex}$$

Here we report the mechanical properties of the pristine and treated CNTF through both methods mentioned above, as shown in and **Table 1** and **Figure 5**. The overall crosslinking process improved the specific tensile strength by 40% from 0.33±0.04 N/tex to 0.46±0.04 N/tex. This does not appear as a remarkable improvement, but if traditional tensile strength is considered, as in many reports [24, 26, 29, 31], the improvement becomes 230% from 70±18 MPa to 232±50 MPa, which is the highest among all reported chemical crosslinking processes. In this study, several factors present in the process can contribute to the improvement of mechanical properties: 1) solvent densification, 2) polymer infiltration, and 3) simultaneous covalent functionalization and crosslinking as discussed above. During solvent evaporation, a capillary force induced by surface tension of the organic solvent brings the CNT bundles closer to each other, which causes the diameter of the fiber to decrease, and results in higher contact

area for enhanced frictional forces [39]. Both Figure 5 (a) and (b) show higher tensile strength of CNTF after being densified by toluene, but there was no significant change on modulus. Impregnation of polymer into the CNTF enhances the CNT junctions through molecular level coupling, which could benefit load transfer between the CNT bundles [21]. The forementioned two factors should be responsible for the improved tensile strength (from 70±18 MPa to 191±41 MPa or from 0.33±0.04 N/tex to 0.43±0.05 N/tex) shown for PS-VBCB infiltrated CNTF after it underwent PS-VBCB infiltration and drying. The infiltrated polymer results in higher stiffness of CNTF as compared to the solvent densified sample, possibly due to the inherent rigidity of polystyrene chains and its derivatives. Excluding this portion of improvement, the additional 93% increase in traditional tensile strength and 10% in specific strength should be attributed to PS-VBCB crosslinking with the CNTF. The covalent functionalization of BCBs onto CNT walls provides strong bondings, while concurrent BCB-BCB coupling results in a reticulate structure that filled the empty spaces between CNT bundles to achieve more effective load transfer.

| | Strength | Modulus | Specific Strength | Specific Modulus |
|-------------------|----------|----------------|-------------------|------------------|
| | (MPa) | (GPa) | (N/tex) | (N/tex) |
| Pristine CNTF | 70±18 | 3.5±2.1 | 0.33 ± 0.04 | 17±4.0 |
| Toluene Densified | 168±25 | 6.6±1.6 | 0.42 ± 0.05 | 17 ± 3.0 |
| CNTF | | | | |
| PS-VBCB | 191±41 | 11.8 ± 2.9 | 0.43 ± 0.05 | 26 ± 3.4 |
| Infiltrated CNTF | | | | |
| PS-VBCB | 256±34 | 15.6 ± 3.0 | 0.46 ± 0.04 | 28 ± 3.5 |
| Crosslinked CNTF | | | | |

Table. 1 Tensile properties of Pristine, Toluene densified, PS-VBCB infiltrated, and PS-VBCB crosslinked CNTF

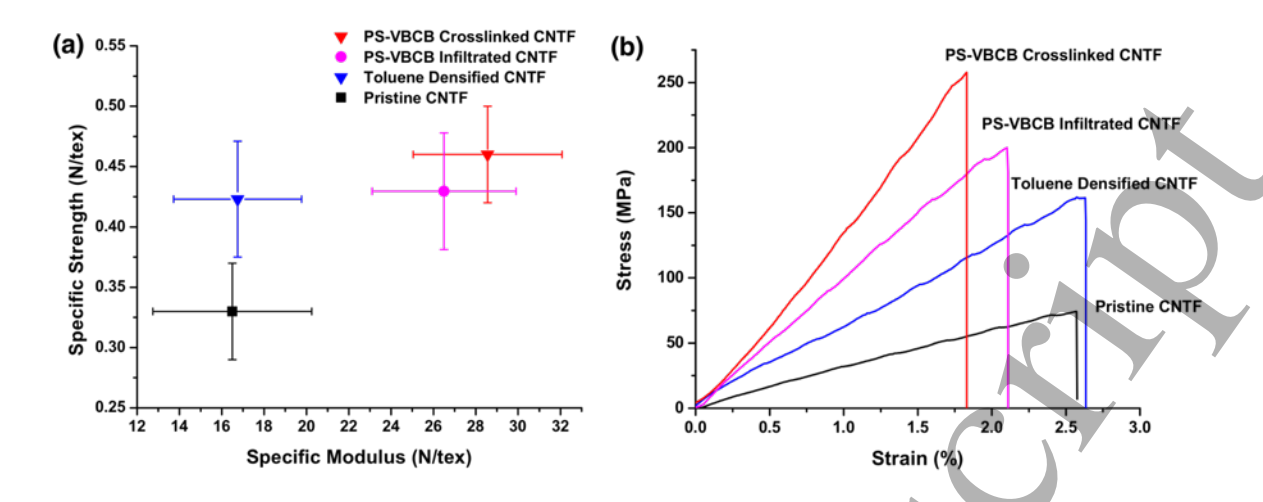


Fig. 5 (a) Specific tensile properties of Pristine, Toluene densified, PS-VBCB infiltrated, and PS-VBCB crosslinked CNTFs with error bars; (b) Typical traditional stress-strain curve of Pristine, Toluene densified, PS-VBCB infiltrated, and PS-VBCB crosslinked CNTF

4. Conclusion

A novel and simple one-step solid-state chemical crosslinking process was developed to improve stiffness and strength of CNTF using a BCB-based polymer. By infiltration of the polymer linker into CNTF followed by heating, covalent functionalization of CNTF with the polymer was achieved with simultaneous inter-CNT crosslinking. Since the CNT bundles were covalently locked in a rigid network, an increase in mechanical properties is observed. The process remarkably improves the specific tensile strength by 40% and traditional tensile strength by 230%. These improvements are not only attributed to the process of polymer infiltration and solvent densification, but are also directly related to simultaneous functionalization and inter-tube linking. This reaction employed required no catalyst, and releases no byproducts. Considering the simplicity of the process with functionalization and covalent crosslinking achieved in a single step, BCB induced crosslinking appears promising for industrial post-treatment of CNTFs to greatly improve their mechanical performance.

Acknowledgement

We are grateful to NASA for funding of this research through an EPSCoR grant to JWM and GB. BCB monomer synthesis and composition characterization of the carbon materials were

carried out conducted at the Center for Nanophase Materials Sciences, which is a DOE Office of Science User Facility. JWM acknowledges a CNMS user project. We thank Conselho Nacional de Desenvolvimento Científico e Tecnológico (CNPq) for Posdoc Scholarship to MCE, and NSF for the UTK REU program for VHR.

References

- [1] R.H. Baughman, C. Cui, A.A. Zakhidov, Z. Iqbal, J.N. Barisci, G.M. Spinks, G.G. Wallace, A. Mazzoldi, D. De Rossi, A.G. Rinzler 1999 Carbon nanotube actuators *Science* **284** 1340-1344
- [2] X. Zhao, B.T. Chu, B. Ballesteros, W. Wang, C. Johnston, J.M. Sykes, P.S. Grant 2009 Spray deposition of steam treated and functionalized single-walled and multi-walled carbon nanotube films for supercapacitors *Nanotechnology* **20** 065605
- [3] J.G. Park, J. Louis, Q. Cheng, J. Bao, J. Smithyman, R. Liang, B. Wang, C. Zhang, J.S. Brooks, L. Kramer 2009 Electromagnetic interference shielding properties of carbon nanotube buckypaper composites *Nanotechnology* **20** 415702
- [4] M.F. De Volder, S.H. Tawfick, R.H. Baughman, A.J. Hart 2013 Carbon nanotubes: present and future commercial applications *Science* **339** 535-539
- [5] K. Jiang, J. Wang, Q. Li, L. Liu, C. Liu, S. Fan 2011 Superaligned carbon nanotube arrays, films, and yarns: A road to applications *Advanced Materials* **23** 1154-1161
- [6] M.T. Byrne, Y.K. Gun'ko 2010 Recent Advances in Research on Carbon Nanotube–Polymer Composites *Advanced Materials* **22** 1672-1688
- [7] M. Zhang, K.R. Atkinson, R.H. Baughman 2004 Multifunctional carbon nanotube yarns by downsizing an ancient technology *Science* **306** 1358-1361
- [8] K. Koziol, J. Vilatela, A. Moisala, M. Motta, P. Cunniff, M. Sennett, A. Windle 2007 High-performance carbon nanotube fiber *Science* **318** 1892-1895
- [9] N. Behabtu, M.J. Green, M. Pasquali 2008 Carbon nanotube-based neat fibers *Nano Today* **3** 24-34
- [10] W. Lu, M. Zu, J.H. Byun, B.S. Kim, T.W. Chou 2012 State of the art of carbon nanotube fibers: opportunities and challenges *Advanced Materials* **24** 1805-1833
- [11] B. Peng, M. Locascio, P. Zapol, S. Li, S.L. Mielke, G.C. Schatz, H.D. Espinosa 2008 Measurements of near-ultimate strength for multiwalled carbon nanotubes and irradiation-induced crosslinking improvements *Nat Nano* **3** 626-631
- [12] N. Behabtu, C.C. Young, D.E. Tsentalovich, O. Kleinerman, X. Wang, A.W. Ma, E.A. Bengio, R.F. ter Waarbeek, J.J. de Jong, R.E. Hoogerwerf 2013 Strong, light, multifunctional fibers of carbon nanotubes with ultrahigh conductivity *Science* **339** 182-186
- [13] M.E. Kozlov, R.C. Capps, W.M. Sampson, V.H. Ebron, J.P. Ferraris, R.H. Baughman 2005 Spinning Solid and Hollow Polymer Free Carbon Nanotube Fibers *Advanced Materials* 17 614-617
- [14] X. Zhang, K. Jiang, C. Feng, P. Liu, L. Zhang, J. Kong, T. Zhang, Q. Li, S. Fan 2006 Spinning and processing continuous yarns from 4 inch wafer scale super aligned carbon nanotube arrays *Advanced Materials* **18** 1505-1510
- [15] Y.-L. Li, I.A. Kinloch, A.H. Windle 2004 Direct spinning of carbon nanotube fibers from chemical vapor deposition synthesis *Science* **304** 276-278
- [16] Y. Wang, G. Colas, T. Filleter 2016 Improvements in the mechanical properties of carbon nanotube fibers through graphene oxide interlocking *Carbon* **98** 291-299
- [17] A.M. Beese, X. Wei, S. Sarkar, R. Ramachandramoorthy, M.R. Roenbeck, A. Moravsky, M. Ford, F. Yavari, D.T. Keane, R.O. Loutfy, S.T. Nguyen, H.D. Espinosa 2014 Key Factors

- Limiting Carbon Nanotube Yarn Strength: Exploring Processing-Structure-Property Relationships *ACS Nano* **8** 11454-11466
- [18] M. Miao 2015 Characteristics of carbon nanotube yarn structure unveiled by acoustic wave propagation *Carbon* **91** 163-170
- [19] L. Qiu, K. Yi-Lan, Q. Wei, L. Ya-Li, H. Gan-Yun, G. Jian-Gang, D. Wei-Lin, Z. Xiao-Hua 2011 Deformation mechanisms of carbon nanotube fibres under tensile loading by in situ Raman spectroscopy analysis *Nanotechnology* **22** 225704
- [20] K. Liu, Y. Sun, R. Zhou, H. Zhu, J. Wang, L. Liu, S. Fan, K. Jiang 2009 Carbon nanotube yarns with high tensile strength made by a twisting and shrinking method *Nanotechnology* **21** 045708
- [21] G. Sakellariou, A. Avgeropoulos, N. Hadjichristidis, J.W. Mays, D. Baskaran 2009 Functionalized organic nanoparticles from core-crosslinked poly(4-vinylbenzocyclobutene-b-butadiene) diblock copolymer micelles *Polymer* **50** 6202-6211
- [22] Y. Jung, T. Kim, C.R. Park 2015 Effect of polymer infiltration on structure and properties of carbon nanotube yarns *Carbon* **88** 60-69
- [23] S.G. Miller, T.S. Williams, J.S. Baker, F. Solá, M. Lebron-Colon, L.S. McCorkle, N.G. Wilmoth, J. Gaier, M. Chen, M.A. Meador 2014 Increased Tensile Strength of Carbon Nanotube Yarns and Sheets through Chemical Modification and Electron Beam Irradiation *ACS Applied Materials & Interfaces* 6 6120-6126
- [24] S. Ryu, Y. Lee, J.W. Hwang, S. Hong, C. Kim, T.G. Park, H. Lee, S.H. Hong 2011 High Strength Carbon Nanotube Fibers Fabricated by Infiltration and Curing of Mussel Inspired Catecholamine Polymer *Advanced Materials* **23** 1971-1975
- [25] S. Boncel, R.M. Sundaram, A.H. Windle, K.K. Koziol 2011 Enhancement of the mechanical properties of directly spun CNT fibers by chemical treatment *ACS nano* **5** 9339-9344
- [26] Y. Cui, M. Zhang 2013 Cross-links in Carbon Nanotube Assembly Introduced by Using Polyacrylonitrile as Precursor *ACS applied materials & interfaces* **5** 8173-8178
- [27] T.Q. Tran, Z. Fan, P. Liu, S.M. Myint, H.M. Duong 2016 Super-strong and highly conductive carbon nanotube ribbons from post-treatment methods *Carbon* **99** 407-415
- [28] T.S. Williams, N.D. Orloff, J.S. Baker, S.G. Miller, B. Natarajan, J. Obrzut, L.S.
- McCorkle, M. Lebron-Colón, J. Gaier, M.A. Meador 2016 Trade-off between the Mechanical Strength and Microwave Electrical Properties of Functionalized and Irradiated Carbon Nanotube Sheets *ACS Applied Materials & Interfaces*
- [29] J. Min, J.Y. Cai, M. Sridhar, C.D. Easton, T. R. Gengenbach, J. McDonnell, W. Humphries, S. Lucas 2013 High performance carbon nanotube spun yarns from a crosslinked network *Carbon* **52** 520-527
- [30] J. Zhang, D. Jiang, H.-X. Peng, F. Qin 2013 Enhanced mechanical and electrical properties of carbon nanotube buckypaper by in situ cross-linking *Carbon* **63** 125-132 [31] Y.-M. Choi, H. Choo, H. Yeo, N.-H. You, D.S. Lee, B.-C. Ku, H.C. Kim, P.-H. Bong, Y. Jeong, M. Goh 2013 Chemical Method for Improving Both the Electrical Conductivity and Mechanical Properties of Carbon Nanotube Yarn via Intramolecular Cross-Dehydrogenative Coupling *ACS Applied Materials & Interfaces* **5** 7726-7730
- [32] M. Miao, S.C. Hawkins, J.Y. Cai, T.R. Gengenbach, R. Knott, C.P. Huynh 2011 Effect of gamma-irradiation on the mechanical properties of carbon nanotube yarns *Carbon* 49 4940-4947
- [33] J. Åström, A. Krasheninnikov, K. Nordlund 2004 Carbon nanotube mats and fibers with irradiation-improved mechanical characteristics: a theoretical model *Physical review letters* **93** 215503
- [34] G. Sakellariou, D. Baskaran, N. Hadjichristidis, J.W. Mays 2006 Well-defined poly (4-vinylbenzocyclobutene): Synthesis by living anionic polymerization and characterization *Macromolecules* **39** 3525-3530

- [35] E. Harth, B.V. Horn, V.Y. Lee, D.S. Germack, C.P. Gonzales, R.D. Miller, C.J. Hawker 2002 A facile approach to architecturally defined nanoparticles via intramolecular chain collapse *Journal of the American Chemical Society* **124** 8653-8660
- [36] G. Sakellariou, H. Ji, J.W. Mays, N. Hadjichristidis, D. Baskaran 2007 Controlled covalent functionalization of multiwalled carbon nanotubes using [4+2] cycloaddition of benzocyclobutenes *Chem Mater* **19** 6370-6372
- [37] G. Sakellariou, H. Ji, J.W. Mays, D. Baskaran 2008 Enhanced polymer grafting from multiwalled carbon nanotubes through living anionic surface-initiated polymerization *Chem Mater* **20** 6217-6230
- [38] A.S. Wu, T.-W. Chou 2012 Carbon nanotube fibers for advanced composites *Materials Today* **15** 302-310
- [39] N. Hiremath, X. Lu, M.C. Evora, A. Naskar, J. Mays, G. Bhat 2016 Effect of solvent/polymer infiltration and irradiation on microstructure and tensile properties of carbon nanotube yarns *Journal of Materials Science* **51** 10215-10228

